



A study of fatigue crack growth laws in small and large cracks based on COD

H. Nisitani, Y. Oda

Faculty of Engineering, Kyushu University, 6-10-1 Hakozaki, Higashi-ku, Fukuoka, 812, Japan

ABSTRACT

Fatigue crack growth tests were carried out on an annealed 0.45% C steel. Crack opening displacement ranges (ΔCOD 's) along a crack were measured in the neighborhood of the crack tip from the SEM photographs taken of positive metal replicas of surface cracks under the maximum and minimum loads. The physical background of the two representative crack growth laws: $dl/dN = C_1 \sigma^n l$ for small cracks under high nominal stresses and $dl/dN = C \Delta K^m$ for large cracks under low nominal stresses, which formally contradict each other, was discussed on the basis of the measured ΔCOD 's. In small and large cracks having the same growth rate, the geometries of measured ΔCOD 's near the crack tips were also almost the same. Therefore, the ΔCOD distribution near the crack tip can be considered as a fundamental factor controlling consistently the growth rate of a crack ranging from small to large cracks.

INTRODUCTION

In the last four decades a large number of fatigue crack growth tests have been carried out and a large number of crack growth laws have been proposed empirically and theoretically [1]. All these laws have succeeded to some degree in describing the crack growth, however, have limitations in the applicable region, and some of these equations formally contradict each other. Therefore, a parameter which can be applicable in the wide range from small to large cracks and from low to high cycle fatigue is desired. Since it can be considered that fatigue crack growth mainly occurs by the accumulation of incremental decohesion of extremely strained material at the crack tip, it is reasonable to use the cyclic crack tip opening displacement $\Delta CTOD$ as a measure of crack growth. Actually, it is successfully used in



48 Localized Damage

explaining the fatigue crack growth of single crystalline metal and alloy [2,3] or a special polycrystalline alloy [4]. However, in general polycrystalline alloys the definition of $\Delta CTOD$ is not clear and difficult to determine. Therefore, the assumption $dl/dN \propto r_{prev}$ (r_{prev} : reversible plastic zone size) was adopted by Nisitani [5] to give a unified explanation of the formal contradiction between the crack growth law for small cracks, Equation (1), proposed by Nisitani [5], and the representative one for large cracks, Paris's law [6], Equation (2):

$$dl/dN = C_1 \sigma^n l \quad (1)$$

$$dl/dN = C \Delta K^m, \quad (2)$$

where σ is the stress amplitude, l is the crack length, and C_1 , C , n and m are constants. Usually, m is about 4 and n is much larger than 2. The assumption was experimentally verified in the special case of a Fe-Si alloy [7].

As for the crack opening displacements, a significant result was obtained based on the measurement of ΔCOD in low-cycle bending fatigue tests on an annealed 0.45% C steel inside the SEM [8]. Surface cracks having the same growth rate but different lengths and different applied strain levels have the same shape of crack opening near the tip. This implies that the ΔCOD near the crack tip is a fundamental factor controlling the crack growth rate. Although this result was obtained from only low-cycle fatigue tests, the similar phenomenon is expected to occur in general in another case of crack growth.

The ΔCOD has an advantage of being measurable in polycrystalline alloys. Therefore, in the present study, the ΔCOD is again treated in rotating bending fatigue tests on a medium carbon steel, but ΔCOD 's are measured in the case of small- and large-crack growths represented by Equation (1) and (2) respectively. The consistent physical background of the above two growth laws is discussed based on the comparisons of measured ΔCOD distributions among the cracks having the same growth rate.

MATERIAL, SPECIMEN AND EXPERIMENTAL PROCEDURES

The material used in this study is a 0.45% carbon steel (JIS S45C) rolled cylindrical bar with a diameter of 19 mm. The chemical composition of this material is as follows: 0.45% C, 0.25% Si, 0.79% Mn, 0.01% P, 0.01% S, 0.09% Cu, 0.03% Ni, 0.18% Cr, and the balance Fe. The specimens were machined after annealing for 1 hour at 845°C. The mechanical properties of the material after annealing are lower yield stress (σ_{sl}) = 364 MPa, ultimate tensile strength (σ_B) = 631 MPa, actual breaking stress (σ_T) = 1156 MPa, reduction of area (ψ) = 45.8 %. The shape and dimensions of the specimen

Table 1: Testing conditions

Specimen No.	σ (MPa)	Growth law to be used
F1	274	$\sigma^n l$
F2	245	$\sigma^n l$
F3	196($\sigma_1 = 274$)	ΔK^m
F4	196($\sigma_1 = 245$)	ΔK^m

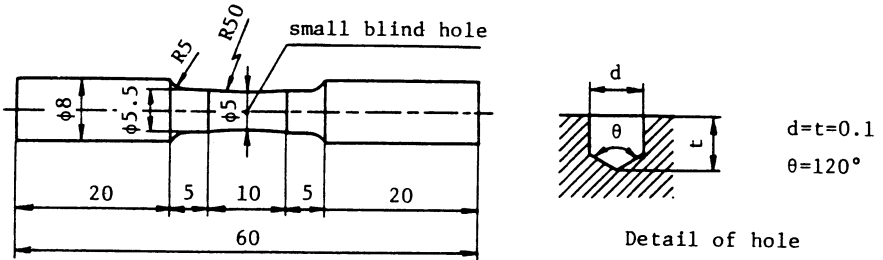


Figure 1: Shape and dimensions (in mm) of the specimen.

are shown in Figure 1. After machining the specimens were reannealed at 600°C for 1 hour in vacuum. Before the fatigue tests, the surface layer with a depth of about 20 μm were electropolished to remove the work-hardened layer and to facilitate the observation of the specimen surface. Then a small blind hole with a diameter of 0.1 mm and a depth of 0.1 mm was drilled at the center of each specimen, as shown in Figure 1. The tests were conducted at a rate of about 3000 rpm using the Ono-type rotating-bending fatigue testing machine with a capacity of 14.7 Nm.

Testing conditions and the crack growth laws predicted from previous study [9] are listed in Table 1. In specimens F3 and F4, in order to investigate the characteristics of crack growth at a low stress amplitude, a pre-crack with a length of approximately 0.5 mm was introduced at a high stress amplitude σ_1 . There is no effect of pre-cracking on growth behavior after the crack reaches at approximately 1 mm, therefore Equation (1) holds [9].

Surface cracks were monitored using a plastic replica method. The crack length along the circumference including the diameter of small hole were measured with an optical microscope. The plastic replicas were gold-coated, copper-plated and finally peeled off, thus we obtained the positive metal replicas appropriate for the SEM observation at high magnifications. The example of SEM photographs of positive metal replicas near the tip

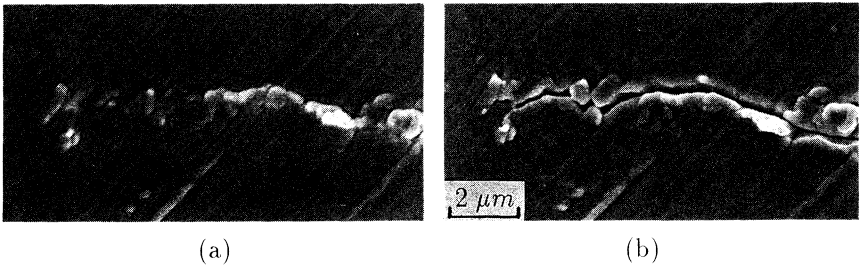


Figure 2: Example of a pair of SEM photographs taken of positive metal replicas (a) at the maximum compression, (b) at the maximum tension.

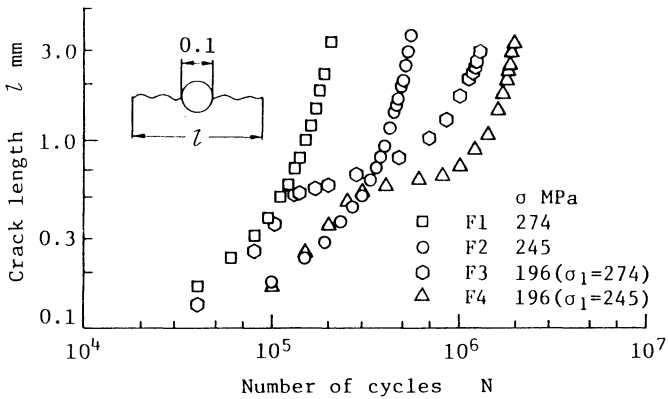


Figure 3: Crack growth curves.

of crack at the maximum compression and tension are shown in Figure 2. Crack opening displacement ranges (ΔCOD 's) were determined from such photographs by measuring the change in distance between each pair of distinctive marks due to electropolishing or stress repetitions or by measuring the amount of each offset of fine pre-scratched parallel lines oriented at 45° to the loading axis.

EXPERIMENTAL RESULTS AND DISCUSSION

Figure 3 shows the crack growth curves on a log-log scale. In specimens F3 and F4, in order to investigate the crack growth behavior at a low stress amplitude, after introducing a pre-crack the stress were changed.

Figure 4 shows the relationship between the crack growth rate dl/dN and the crack length l on a log-log scale. As can be seen in Figure 4, each early stage of $\log dl/dN - \log l$ curves under a high stress amplitude: 245 or

274 MPa, reveals a linear relation with a slope of unity. This means that the crack growth rate is proportional to the crack length. Furthermore, dl/dN in this stage is also proportional to $\sigma^{7.5}$. Consequently, as can be seen in Figure 5, a plot of $\log dl/dN$ against $\log \sigma^{7.5}$ reveals a linear relation with a slope of unity. The relation is independent of applied stress levels. Therefore, the growth rates of small cracks under high stress amplitudes can be uniquely determined by Equation (1).

Figure 6 shows the relationship between dl/dN and ΔK on a log-log scale in the case of $\sigma = 196$ MPa. Stress intensity factors near the surface were determined from the solution by Shiratori [7] for a semi-elliptical surface crack with an aspect ratio of 0.8 [8] in a bar under bending. The slope is approximately 4. Therefore, the crack growth rate may be represented by Equation (1) as described in Reference 11.

Figure 7 shows the comparisons among the measured ΔCOD distributions near the tips of cracks having the same growth rate but different crack lengths and different applied stress levels. In Figures 7(a) and (b), the crack growth rates are different; that is, $dl/dN = 2.5 \times 10^{-6}$ and 7.5×10^{-6} mm/cycle, respectively. In Figure 7(a), the ΔCOD distributions are almost the same, notwithstanding marks \circ and \triangle indicate the ΔCOD 's of cracks controlled by different growth laws: Equation (1) for a small crack under a high stress amplitude and Equation (2) for a large crack under a low stress amplitude. Similar phenomena can be also seen in Figure 7(b), where marks \square , \circ and a mark \triangle indicate the ΔCOD 's of cracks controlled by Equations (1) and (2), respectively. Thus, cracks having the same growth rate show the same shape of crack opening near the tip, in spite of different crack lengths and different applied stress levels. It means that the ΔCOD distribution near the crack tip can be considered as a fundamental factor controlling the growth rate of a crack ranging from small to large cracks.

CONCLUSIONS

Rotating bending fatigue tests on an annealed 0.45% C steel were carried out. The ΔCOD distribution has the advantage of being measurable even in polycrystalline alloys, therefore were measured on the surface of specimens. The physical background of the two fatigue growth laws in small and large surface cracks, Equation (1) and (2), which formally contradict each other, was discussed on the basis of the measured ΔCOD 's. Cracks having the same growth rate have almost the same distribution of ΔCOD near the crack tip, independently of crack lengths and applied stress levels. Therefore, the ΔCOD distribution near the crack tip can be considered as a fundamental factor controlling the crack growth rate of a surface crack ranging from small to large cracks.

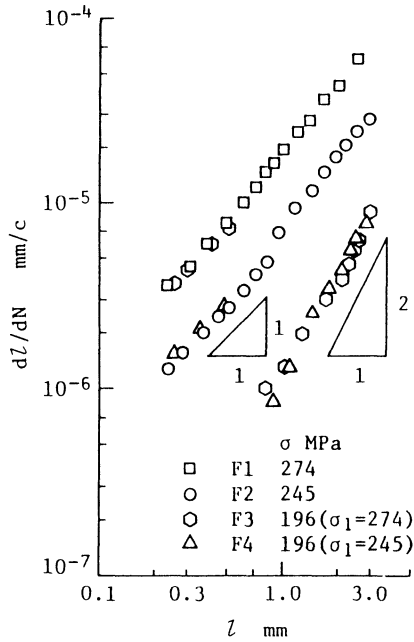


Figure 4: Relationship between crack growth rate and crack length.

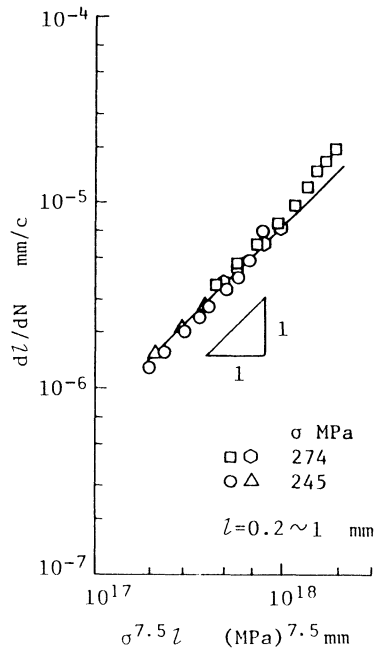


Figure 5: Relationship between crack growth rate and $\sigma^{7.5}l$ in the case of small cracks under high stress amplitudes.

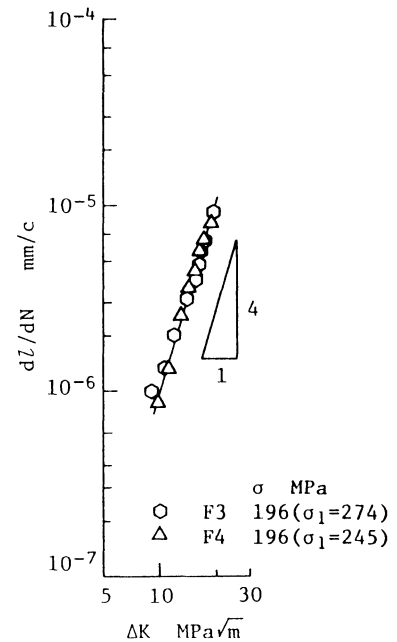


Figure 6: Relationship between crack growth rate and stress intensity factor range in the case of large cracks under a low stress amplitude.

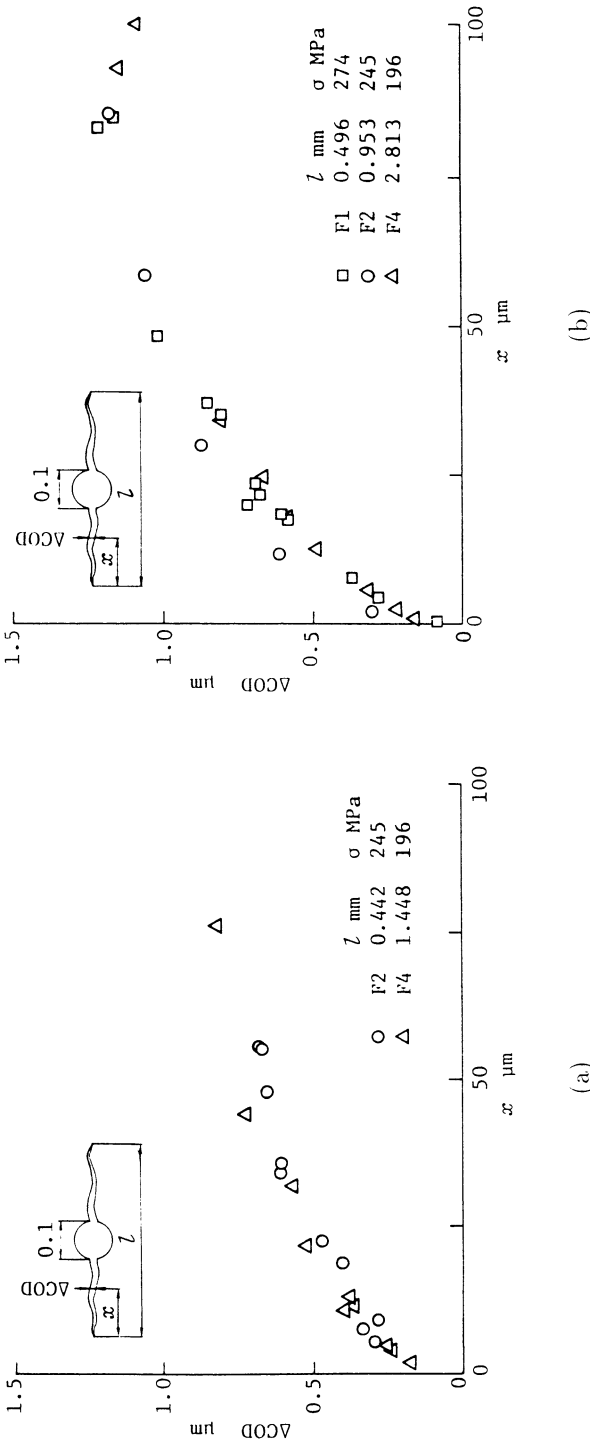


Figure 7: Crack opening displacement ranges in the case of cracks having the same growth rate but different crack lengths and different applied stress levels; (a) at $dl/dN \approx 2.5 \times 10^{-6}$ mm/cycle, (b) at $dl/dN \approx 7.5 \times 10^{-6}$ mm/cycle.



REFERENCES

1. For example, Kocanda, S., *Fatigue Failure of Metals* Sijthoff & Noordhoff Inter. Publishers, 1978.
2. Neumann, P., 'New Experiments Concerning the Slip Processes at Propagating Fatigue Crack-I', *Acta. Metall.*, Vol. 22, pp. 1155-1165, 1974.
3. Neumann, P., Vehoff, H. and Fuhlrott, H., 'On the Mechanisms of Fatigue Crack Growth', Vol. 2, pp. 1313-1324, *Proceedings of the 4th Int. Conf. on Fracture*, 1977.
4. Kikukawa, M., Jono, M. and Adachi, M., 'Direct Observation of Fatigue Crack by Scanning Electron Microscope and Its Propagation Mechanism' *J. Soc. Mater. Sci. Jpn.*, (in Japanese), Vol. 27, pp. 853-858, 1978.
5. Nisitani, H., 'Unifying Treatment of Fatigue Crack Growth Laws in Small, Large and Non-Propagating Cracks' *Mechanics of Fatigue* ed. Mura, T. AMD-Vol. 47, pp. 151-166, ASME, 1981.
6. Paris, P.C. and Erdogan, F., 'A Critical Analysis of Crack Propagation Laws' *Trans. ASME, Ser. D*, Vol. 85, No. 4, pp. 528-534, 1963.
7. Nisitani, H. and Kawagoishi, N., 'Relation Between Fatigue Crack Growth Law and Reversible Plastic Zone Size in Fe-3%Si Alloy' pp. 795-800, *Proc. 6th Int. Cong. on Exp. Mech.* Vol. 2, 1988.
8. Nisitani, H., Oda, Y. and Yakushiji, T., 'Considerations of the Small-Crack Growth Law Based on COD (Low-Cycle Bending Fatigue Test of an Annealed 0.45%C Steel in the SEM)', *JSME International Journal*, Ser. I, Vol. 33, No. 2, pp. 243-248, 1990.
9. Nisitani, H. and Goto, M., 'Investigation of Miner's Rule Based on the Behavior of Micro-Cracks: Rotating Bending of an Annealed 0.45%C Steel', *Trans. Jpn. Soc. Mech. Eng.*, (in Japanese), Vol. 49, No. 443, A, pp. 779-787, 1983.
10. Nisitani, H., Goto, M. and Kawagoishi, N., 'Comparison of Fatigue Crack Growth Laws under a High Nominal and a Low Nominal Stress (Fully-Reversed Tension-Compression of an Annealed 0.45%C Steel)', *Trans. Jpn. Soc. Mech. Eng.*, (in Japanese), Vol. 50, No. 449, A, pp. 23-32, 1984.
11. Shiratori, M., Miyoshi, T., Sakai, Y. and Zhang, G.-R., 'Analysis of Stress Intensity Factors for Surface Cracks Subjected to Arbitrarily Distributed Surface Stresses (3rd Report, Analysis and Application of Influence Coefficients for Round Bars with a Semielliptical Surface Crack)' *Trans. Jpn. Soc. Mech. Eng.*, (in Japanese), Vol. 53, No. 488, A, pp. 779-785, 1987.
12. Nisitani, H., Kawagoishi, N. and Wakahara, M., 'Comparison of Fatigue Processes between Rotating Bending and Plane Bending in an Annealed Steel' *J. Soc. Mater. Sci. Jpn.*, (in Japanese), Vol. 33, pp. 311-316, 1984.